The Canadian Mineralogist
Vol. 39, pp. 797-807 (2001)

STRUCTURE TOPOLOGY AND HYDROGEN BONDING IN MARTHOZITE, $Cu^{2+}[(UO_2)_3(SeO_3)_2O_2](H_2O)_8$, A COMPARISON WITH GUILLEMINITE, $Ba[(UO_2)_3(SeO_3)_2O_2](H_2O)_3$

MARK A. COOPER AND FRANK C. HAWTHORNE§

Department of Geological Sciences, University of Manitoba, Winnipeg, Manitoba R3T 2N2, Canada

ABSTRACT

The crystal structure of marthozite, Cu^{2+} $[(UO_2)_3$ $(SeO_3)_2$ $O_2]$ $(H_2O)_8$, *a* 6.9879(4), *b* 16.4537(10), *c* 17.2229(10) Å, *V* 1980.2(3) Å^3, *Pbn*2$_1$, *Z* = 4, D_{calc} = 4.37 g/cm^3, has been solved by direct methods and refined to an *R* index of 5.7% for 4364 observed ($|F_o| > 4\sigma F$) reflections collected with a four-circle diffractometer fitted with Mo*K*α X-radiation and a CCD detector. There are three unique *U* sites, each occupied by U^{6+} with two short *U*–O_{uranyl} bonds (1.76–1.82 Å) and coordination numbers of [8], [7] and [7], respectively. There are two unique *Se* sites, each occupied by Se^{4+} and coordinated by three O atoms (*Se*–O ≈ 1.70 Å), forming a triangular pyramid with Se at the apex, indicative of stereoactive lone-pair behavior in Se^{4+}. There is one *Cu* site, occupied by Cu^{2+} in octahedral coordination by four (H_2O) groups (*Cu*–H_2O ≈ 2.0 Å) and two O atoms (*Cu*–O ≈ 2.4 Å). The structural unit is a sheet of composition $[(UO_2)_3$ $(SeO_3)_2$ $O_2]$, comprised of chains of edge-sharing ($U\phi_n$) polyhedra extending along [100] that are cross-linked in the [001] direction by (SeO_3) groups; this sheet is topologically identical to the structural unit in guilleminite, Ba $[(UO_2)_3$ $(SeO_3)_2$ $O_2]$ $(H_2O)_3$. Adjacent sheets are linked through interstitial Cu^{2+} cations *via* Cu^{2+}–O_{apical} bonds and *via* H bonds that involve both (H_2O) groups bonded to Cu^{2+} and interstitial (H_2O) groups not bonded to any cation.

The principal differences between marthozite and guilleminite involve the interlayer species. In guilleminite, the Ba atom is centrally positioned with respect to the chain of (UO_n) polyhedra, whereas in marthozite, the Cu^{2+} atom is located off the pseudo-mirror plane of the chain of (UO_n) polyhedra. This differential positioning of the interstitial cations results in an intersheet separation in marthozite that is nearly 1 Å greater than that in guilleminite, despite the fact that Ba (in guilleminite) is much larger than Cu^{2+} (in marthozite). The H-bond arrangement in marthozite is very different from that in guilleminite. In marthozite, there are eight unique interlayer (H_2O) groups; four of these (H_2O) groups bond directly to Cu^{2+} and four are held in the structure solely by H bonds. In guilleminite, there are two unique interlayer (H_2O) groups, both of which bond to the interlayer Ba atoms.

Keywords: marthozite, crystal structure, chemical formula, hydrogen bonding, uranium mineral, guilleminite.

SOMMAIRE

Nous avons résolu la structure cristalline de la marthozite, Cu^{2+} $[(UO_2)_3$ $(SeO_3)_2$ $O_2]$ $(H_2O)_8$, *a* 6.9879(4), *b* 16.4537(10), *c* 17.2229(10) Å, *V* 1980.2(3) Å^3, *Pbn*2$_1$, *Z* = 4, D_{calc} = 4.37 g/cm^3, par méthodes directes, nous l'avons affiné jusqu'à un résidu R de 5.7% pour 4364 réflexions observées ($|F_o| > 4\sigma F$) prélevées avec un diffractomètre à quatre cercles (rayonnement Mo*K*α) muni d'un détecteur de type CCD. Il y a quatre sites *U* uniques, chacun étant occupé par un atome U^{6+} avec deux courtes liaisons *U*–$O_{uranyle}$ (1.76–1.82 Å) et une coordinence de [8], [7] et [7], respectivement. Il y a deux sites *Se* uniques, chacun occupé par un atome Se^{4+} en coordinence avec trois atomes d'oxygène (*Se*–O ≈ 1.70 Å), formant une pyramide triangulaire ayant le Se à son sommet, indication d'un comportement de paires d'électrons isolés stéréoactifs sur l'ion Se^{4+}. Il y a un site *Cu*, occupé par le Cu^{2+} en coordinence octaédrique par quatre groupes H_2O (*Cu*–H_2O ≈ 2.0 Å) et deux atomes d'oxygène (*Cu*–O ≈ 2.4 Å). L'unité structurale est un feuillet ayant la composition $[(UO_2)_3$ $(SeO_3)_2$ $O_2]$, comportant des chaînes de polyèdres ($U\phi_n$) à arêtes partagées alignées le long de [100] qui sont liées transversalement dans la direction [001] par des groupes (SeO_3); ce feuillet est topologiquement identique à l'unité structurale de la guilleminite, Ba $[(UO_2)_3$ $(SeO_3)_2$ $O_2]$ $(H_2O)_3$. Les feuillets adjacents sont rattachés par des cations interstitiels Cu^{2+} grâce à des liaisons Cu^{2+}–O_{apical} et à des liaisons hydrogène impliquant à la fois des groupes (H_2O) liés aux cations Cu^{2+} et des groupes (H_2O) interstitiels non liés à ce cation.

Les différences principales entre la marthozite et la guilleminite impliquent l'espèce interstitielle. Dans la guilleminite, l'atome Ba adopte une position centrale par rapport à la chaîne de polyèdres (UO_n), tandis dans la marthozite, l'atome Cu^{2+} est deplacé par rapport au plan du pseudo-miroir de la chaîne des polyèdres (UO_n). Cette différence en position des cations interstitiels mène à une séparation inter-feuillet supérieure à celle dans la guilleminite de presque 1 Å, malgré le fait que le Ba (dans la guilleminite) ait un rayon ionique beaucoup supérieur à celui du Cu^{2+} (dans la marthozite). Les réseaux des liaisons hydrogène dans la marthozite

§ *E-mail address*: frank_hawthorne@umanitoba.ca

et la guilleminite diffèrent de façon importante. Dans la marthozite, il y a huit groupes (H_2O) interfoliaires uniques; quatre de ceux-ci entrent en liaison directe avec le Cu^{2+}, et quatre sont maintenus dans la structure uniquement par des liaisons hydrogène. Dans la guilleminite, il y a deux groupes (H_2O) interfoliaires uniques, les deux étant liés aux atomes Ba interfoliaires.

(Traduit par la Rédaction)

Mots-clés: marthozite, structure cristalline, formule chimique, liaison hydrogène, minéral d'uranium, guilleminite.

Introduction

We initiated a structural study of marthozite while working on the crystal structure of guilleminite, Ba $[(UO_2)_3\ (SeO_3)_2\ O_2]\ (H_2O)_3$ (Cooper & Hawthorne 1995). We have examined several crystals of marthozite during the past five years, and all have the unit cell of "metamarthozite" (Cesbron *et al.* 1969), which has a 15.8 Å repeat-distance perpendicular to the principal cleavage. In all cases, only a partial structure was recoverable, indicating that the structural unit is a sheet of probable composition $[(UO_2)_3\ (SeO_3)_2\ O_2]$, the same sheet that is the structural unit in the guilleminite structure (Cooper & Hawthorne 1995). The chemical formula reported by Cesbron *et al.* (1969) for fully hydrated marthozite (a 16.4 Å repeat-distance perpendicular to the cleavage direction) is $Cu\ (UO_2)_3\ (SeO_3)_3\ (OH)_2\ (H_2O)_7$. As part of a continuing study of marthozite, we were fortunate to acquire a sample containing superior crystals of fully hydrated marthozite; we report here its crystal structure.

Experimental

The fine crystals used in this study are from the Musonoi mine, Shaba Province, Democratic Republic of Congo, and were generously provided for this study by Mr. William Pinch. A platy crystal (Table 1), bounded by morphological faces, was mounted on a Bruker four-circle diffractometer equipped with a 1K CCD detector at a crystal-to-detector distance of 4 cm. As was pointed out by Burns (1998), CCD data-collection strategy can be optimized for highly absorbing crystals by taking into account the shape and orientation of the crystal. We are not yet aware of any published account of such an optimized strategy for highly absorbing crystals, and present here a detailed account of our data-collection procedure. We note that the following strategy is for an automated four-circle diffractometer with total freedom in ψ; this specific strategy is not applicable to a three-circle diffractometer, which has fewer degrees of freedom.

An important aspect to CCD data-acquisition is that no unit cell is required to collect the data; this is a double-edged sword in that one can mount any crystal and collect intensity data regardless of crystal suitability. In this regard, we have developed a set of five preliminary frame-sequences in order to assess crystal quality and help select suitable frame-widths and frame-times. Reciprocal space is sampled in a mutually orthogonal fashion over 6 to 25° of scan angle, depending upon average spot-size and population of reflections in a frame. For marthozite, analysis of the three-dimensional shapes of spots from these initial frames showed that we had a single crystal of high quality, and reflections taken from these frames gave a unit cell corresponding to fully hydrated marthozite. The 60 s frame-time used for these initial frames is sufficient to give observed reflections to the edge of the frame (60° 2θ). More than a sphere of intensity data was then collected with nine data-runs, using a frame width of 0.2° and a frame time of 60 s. The data runs were designed with the simulation program ASTRO, and use both ϕ and ω as scan axes. Users can e-mail the senior author for a list of data runs, accompanying software collision-limits and telescope setting. The following geometrical relations are important in conjunction with the nine data-runs for moderately to highly absorbing crystals of platy morphology: (1) thin plates are mounted vertically onto the end of a glass fiber; (2) the goniometer head is manually rotated around the ϕ axis until the plane of the crystal plate is parallel to the line-of-sight of the telescope. From this easily reproducible starting configuration, intensity data for any thin plate can be acquired using the nine data-runs with a guarantee of complete data-coverage and adequate treatment of absorption. This guarantee stems from the following points: (1) multiple ψ-settings are used; (2) the angle between the beam axis and plate surface is maximized during design of the data runs (a very high proportion of unique data is acquired outside a plate-glancing angle of 20°, even in triclinic symmetry); (3) in addition to complete coverage of the

TABLE 1. MISCELLANEOUS INFORMATION FOR MARTHOZITE

a (Å)	6.9879(4)	crystal size (mm)	0.108 x 0.090 x 0.020
b	16.4537(10)	radiation	Mo$K\alpha$/Gr
c	17.2229(10)	No. of reflections	33899
V (Å^3)	1980.2(3)	No. in Ewald sphere	19305
Sp. Gr.	$Pbn2_1$	No. unique	5759
Z	4	No. $\lvert F_o\rvert > 4\sigma(\lvert F_o\rvert)$	4364
μ (mm^{-1})	29.3	R_{merge} %	7.4
D_{meas} * (g/cm^3)	4.4	R_1 ($\lvert F_o\rvert > 4\sigma$) %	5.7
D_{calc} (g/cm^3)	4.37	wR_2 (F_o^2) %	8.0
min/max.	0.0701 / 0.5590		
Cell content	4 [Cu^{2+} ($U^{6+}O_2$)$_3$ ($Se^{4+}O_3$)$_2$ O_2 (H_2O)$_6$]		

$R = \Sigma(\lvert F_o - F_{c_1}\rvert) / \Sigma\ F_o\rvert$

$wR = [\Sigma w(F_o^2 - F_c^2)^2 / \Sigma w(F_o^2)^2]^{\frac{1}{2}}$, $w = 1 / \sigma F_o^2$

* from Cesbron *et al.* (1969)

Ewald sphere, four of the nine data-runs were specifically designed to sample redundant data (ψ sampling) in regions of maximum and minimum transmission (to provide appropriate information for adequate empirical absorption-corrections).

After collection of all nine data-runs, frame sequences uniformly distributed through the entire dataset were sampled to give intense reflections (~1000) for least-squares refinement of the cell dimensions and orientation matrix. The resulting orientation matrix was then fed into the SAINT program for three-dimensional integration of the intensity data, and standard corrections (for Lorentz, polarization and background effects) were applied. The final unit-cell parameters (Table 1) are based on least-squares refinement of 7,317 reflections ($> 10\ \sigma I$). The interactive on-screen face-indexing facility in the SMART program was then used to index all of the crystal faces on the marthozite crystal, and a numerical absorption-correction (using Gaussian quadrature integration) was applied to all 33,899 reflections. Identical reflections (at different Ψ angles) were combined to give a total of 19,305 reflections in the Ewald sphere. In the space group $Pbn2_1$, this gives 5,759 unique data with a Laue (*mmm*) merging of 6.9% (Friedel pairs were not merged).

Structure Solution and Refinement

Scattering curves for neutral atoms, together with anomalous dispersion corrections, were taken from *International Tables for X-ray Crystallography* (1992). The Bruker SHELXTL Version 5 system of programs was used for solution and refinement of the crystal structure. Systematic absences are consistent with space groups $Pbn2_1$ and *Pbnm*; the structure was solved in $Pbn2_1$ using direct methods. Successive cycles of difference-Fourier synthesis and refinement gave the positions of all non-H atoms. Full-matrix least-squares refinement (based on F_o^2 and all 5,759 unique data) of all variable parameters for a model involving anisotropic displacement of the cations and isotropic displacement of the anions converged to an R_1 index of 5.7% for 4,364 observed unique reflections ($|F_o| > 4\sigma F$). A weighting scheme based on $1/\sigma F_o^2$ gave $wR_2 = 8.0\%$. The absolute structural configuration was clearly established [Flack parameter = 0.06(1)]. Final atom parameters are listed in Table 2, and selected interatomic distances and angles are given in Table 3; bond valences are shown in Tables 4 and 5, and details of the proposed H bonds are given in Table 6. Observed and calculated structure-factors may be obtained from The Depository

TABLE 2. FINAL ATOM PARAMETERS FOR MARTHOZITE

	x	*y*	*z*	U_{eq}	U_{11}	U_{22}	U_{33}	U_{23}	U_{13}	U_{12}
U(1)	0.20563(9)	0.27827(7)	0.5	0.0137(2)	0.0098(3)	0.0155(4)	0.0157(3)	0.0012(2)	0.0081(4)	0.0018(5)
U(2)	0.20222(12)	0.20848(6)	0.10493(6)	0.0120(2)	0.0101(3)	0.0148(4)	0.0111(3)	-0.0007(3)	0.0073(4)	-0.0006(4)
U(3)	0.21002(11)	0.23414(5)	0.89322(6)	0.0139(2)	0.0116(3)	0.0189(4)	0.0112(3)	0.0017(3)	0.0075(4)	0.0032(4)
Se(1)	0.1920(3)	0.2877(2)	0.2989(1)	0.0160(4)	0.0097(9)	0.0243(9)	0.0139(9)	-0.0009(8)	0.0060(8)	-0.0006(12)
Se(2)	0.1917(3)	0.3239(1)	0.6966(1)	0.0149(4)	0.0061(8)	0.0261(12)	0.0125(8)	-0.0007(7)	0.0059(8)	0.0031(11)
Cu	0.1976(4)	0.4622(1)	0.1177(1)	0.0231(5)	0.0225(11)	0.0236(13)	0.0232(11)	-0.0012(9)	0.0056(11)	0.0003(13)
O(1)	0.2325(16)	0.2038(7)	0.2441(6)	0.0173(28)						
O(2)	0.0497(16)	0.2466(8)	0.3718(6)	0.0170(27)						
O(3)	0.3861(18)	0.2959(9)	0.3560(7)	0.0294(33)						
O(4)	0.2478(16)	0.2434(8)	0.7561(7)	0.0197(29)						
O(5)	0.0458(15)	0.2800(7)	0.6307(6)	0.0156(27)						
O(6)	0.3748(16)	0.3244(8)	0.6332(6)	0.0189(28)						
O(7)	0.1670(14)	0.3856(8)	0.4888(7)	0.0150(27)						
O(8)	0.2510(14)	0.1709(9)	0.5119(6)	0.0189(33)						
O(9)	0.2493(15)	0.0998(8)	0.0994(7)	0.0167(28)						
O(10)	0.1530(15)	0.3148(7)	0.1211(6)	0.0115(27)						
O(11)	0.2613(16)	0.1287(7)	0.8847(7)	0.0196(29)						
O(12)	0.1649(18)	0.3396(9)	0.8949(7)	0.0270(31)						
O(13)	0.3824(12)	0.2460(6)	0.0030(7)	0.0116(22)						
O(14)	0.5155(12)	0.2948(7)	0.4966(8)	0.0125(22)						
OW(1)	-0.0016(17)	0.4661(8)	0.0303(7)	0.0226(30)						
OW(2)	0.3721(19)	0.4501(8)	0.2062(7)	0.0307(32)						
OW(3)	-0.0051(18)	0.4934(9)	0.1901(7)	0.0250(31)						
OW(4)	0.3993(20)	0.4242(9)	0.0456(7)	0.0372(36)						
OW(5)	0.7045(21)	0.3910(9)	0.1679(7)	0.0342(32)						
OW(6)	0.0287(22)	0.5091(11)	0.3466(9)	0.0471(43)						
OW(7)	0.5051(22)	0.4243(10)	0.7889(7)	0.0385(39)						
OW(8)	0.4841(18)	0.4867(10)	0.4276(8)	0.0412(39)						

TABLE 3. BOND DISTANCES (Å) FOR MARTHOZITE

U(1)–O(7)	1.80(1)	*U*(2)–O(9)	1.82(1)
U(1)–O(8)	1.81(1)	*U*(2)–O(10)	1.80(1)
U(1)–O(2)	2.52(1)	*U*(2)–O(1)	2.41(1)
U(1)–O(3)	2.80(1)	*U*(2)–O(5)b	2.45(1)
U(1)–O(5)	2.51(1)	*U*(2)–O(6)a	2.40(1)
U(1)–O(6)	2.69(1)	*U*(2)–O(13)	2.25(1)
U(1)–O(13)c	2.29(1)	*U*(2)–O(14)a	2.28(1)
U(1)–O(14)	2.18(1)	<*U*(2)–O_{ap}>	1.81
<*U*(1)–O_{ap}>	1.80	<*U*(2)–O_{eq}>	2.36
<*U*(1)–O_{eq}>	2.50		
Cu–O(9)f	2.32(1)	*U*(3)–O(11)	1.78(1)
Cu–O(10)	2.45(1)	*U*(3)–O(12)	1.76(1)
Cu–OW(1)	2.05(1)	*U*(2)–O(2)d	2.42(1)
Cu–OW(2)	1.96(1)	*U*(3)–O(3)c	2.40(1)
Cu–OW(3)	1.96(1)	*U*(3)–O(4)	2.38(1)
Cu–OW(4)	1.98(1)	*U*(3)-O(13)e	2.25(1)
<*Cu*–O_{ap}>	2.38	*U*(3)–O(14)c	2.29(1)
<*Cu*–O_{eq}>	1.99	<*U*(3)–O_{ap}>	1.77
		<*U*(3)–O_{eq}>	2.35
Se(1)–O(1)	1.70(1)	*Se*(2)–O(4)	1.72(1)
Se(1)–O(2)	1.74(1)	*Se*(2)–O(5)	1.69(1)
Se(1)–O(3)	1.68(1)	*Se*(2)–O(6)	1.68(1)
<*Se*(1)–O>	1.71	<*Se*(2)–O>	1.70

a: $x-½$, $\bar{y}+½$, $z-½$; b: $x+½$, $\bar{y}-½$, $z-½$; c: $x-½$, $\bar{y}+½$, $z+½$; d: $x+½$, $\bar{y}+½$, $z+½$; e: x, y, $z+1$; f: $x+½$, $y+½$, z; g: x, $y+1$, $z-½$; h: $\bar{x}+1$, $\bar{y}+1$, $z+½$; i: $x-1$, y, z; j: $x+1$, $\bar{y}+1$, $z-½$

of Unpublished Data, CISTI, National Research Council, Ottawa, Ontario K1A 0S2, Canada.

Chemical Formula

Cesbron *et al.* (1969) reported the formula of fully hydrated marthozite as Cu $(UO_2)_3$ $(SeO_3)_3$ $(OH)_2$ $(H_2O)_7$. As is apparent from Table 2, the U:Se ratio in marthozite is 3:2, and all H atoms in the structure are associated with eight (H_2O) groups; this is in accord with local bond-valence sums (Table 4) and satisfies the requirement of overall electroneutrality. Hence the formula for marthozite is Cu^{2+} $[(UO_2)_3 (SeO_3)_2 O_2] (H_2O)_8$. This gives a calculated density of 4.37 g/cm^3, in good agreement with the measured value of 4.4 g/cm^3 (Cesbron *et al.* 1969).

Cesbron *et al.* (1969) noted a small deficiency in Cu content in their chemical composition relative to their ideal formula. Site-occupancy refinement at the *Cu* site gave full occupancy by Cu, giving one Cu^{2+} *apfu* (atom per formula unit). The chemical composition of the sheet (structural unit) is the same for both marthozite and guilleminite. The two minerals differ in their interlayer compositions: Ba is coordinated by three (H_2O) groups in guilleminite, and Cu is coordinated by four (H_2O) groups [with four additional (H_2O) groups] in marthozite.

TABLE 4. BOND-VALENCE TABLE FOR MARTHOZITE*

	U(1)	*U*(2)	*U*(3)	*Cu*	*Se*(1)	*Se*(2)	Σ	H1A	H1B	H2A	H2B	H3A	H3B	H4A	H4B	H5A	H5B	H6A	H6B	H7A	H7B	H8A	H8B	Σ
O(1)		0.49			1.35		1.84													0.2				2.04
O(2)	0.39		0.48		1.21		2.08																	2.08
O(3)	0.22		0.50		1.42		2.14																	2.14
O(4)			0.52			1.28	1.80									0.2								2.00
O(5)	0.40	0.45				1.39	2.24																	2.24
O(6)	0.28	0.50				1.42	2.20																	2.20
O(7)	1.61						1.61	0.2														0.1		1.91
O(8)	1.58						1.58		0.1						0.1		0.1							1.88
O(9)		1.56		0.18			1.73																	1.73
O(10)		1.62		0.12			1.74																	1.74
O(11)			1.68				1.68											0.1				0.1		1.88
O(12)			1.75				1.75												0.1					1.85
O(13)	0.61	0.67	0.67				1.95																	1.95
O(14)	0.76	0.63	0.62				2.01																	2.01
OW(1)				0.37			0.37	0.8	0.9															2.07
OW(2)				0.47			0.47			0.8	0.8													2.07
OW(3)				0.47			0.47					0.8	0.8											2.07
OW(4)				0.44			0.44							0.8	0.9									2.14
OW(5)							0.00			0.2		0.2				0.8	0.9							2.10
OW(6)							0.00						0.2					0.9	0.9					2.00
OW(7)							0.00				0.2									0.8	0.8		0.2	2.00
OW(8)							0.00							0.2							0.2	0.8	0.8	2.00
Σ	5.85	5.91	6.22	2.05	3.98	4.09		1.0	1.0	1.0	1.0	1.0	1.0	1.0	1.0	1.0	1.0	1.0	1.0	1.0	1.0	1.0	1.0	

* Bond-valence curves, U–O: Burns *et al.* (1997), Cu–O, Se–O: Brown & Altermatt (1985)

TABLE 5. BOND-VALENCE TABLE FOR GUILLEMINITE*

	U(1)	U(2)	Ba	Se	Σ	H1A	H1B	H2A	H2B	Σ
O(1)	1.65		0.19		1.84	0.20				2.04
O(2)	0.50	0.62[×2]	0.17		2.01					2.01
O(3)	0.64	0.68[×2]			2.00					2.00
O(4)	1.61		0.13		1.77		0.10			1.87
O(5)		1.68	0.10[×2]		1.87			0.05		1.92
O(6)		1.59	0.10[×2]		1.78			0.05		1.83
O(7)	0.33[×3]	0.51		1.35	2.19					2.19
O(8)		0.43		1.42	1.91				0.10	2.01
O(9)	0.32[×3]	0.48		1.50	2.30					2.30
W(1)			0.33		0.30	0.80	0.90			2.00
W(2)			0.20[×2]		0.20			0.90	0.90	2.00
Σ	5.80	6.05	1.88	4.27		1.00	1.00	1.00	1.00	

* Bond-valence curves: U–O: Burns *et al.* (1997); Ba–O, Se–O: Brown & Altermatt (1985).

TABLE 6. PROPOSED H-BONDING FOR MARTHOZITE AND GUILLEMINITE

marthozite			
OW(1)–H1A....O(7)g	2.79(2) Å	O(7)g–OW(1)–O(8)a	114.2(5)°
OW(1)–H1B.....O(8)a	2.86(2)		
OW(2)–H2A.....OW(5)	2.80(2)	OW(5)–OW(2)–OW(7)j	98.0(6)
OW(2)–H2B.....OW(7)j	2.65(2)		
OW(3)–H3A.....OW(5)i	2.67(2)	OW(5)i–OW(3)–OW(6)	105.6(6)
OW(3)–H3B.....OW(6)	2.72(2)		
OW(4)–H4A.....OW(8)j	2.64(2)	OW(8)j–OW(4)–O(8)b	83.5(5)
OW(4)–H4B.....O(8)b	2.97(2)		
OW(5)–H5A.....O(4)b	2.70(2)	O(4)b–OW(5)–O(8)b	102.8(6)
OW(5)–H5B.....O(8)b	2.89(2)		
OW(6)–H6A.....O(11)a	3.01(2)	O(11)a–OW(6)–O(12)g	106.8(6)
OW(6)–H6B.....O(12)g	2.95(2)		
OW(7)–H7A.....O(1)d	2.75(2)	O(1)d–OW(7)–OW(8)h	128.6(6)
OW(7)–H7B.....OW(8)h	2.80(2)		
OW(8)–H8A.....O(7)	2.97(2)	O(7)–OW(8)–OW(7)j	128.1(6)
OW(8)–H8A.....O(11)b	2.81(2)	O(11)b–OW(8)–OW(7)j	96.4(6)
OW(8)–H8B.....OW(7)j	2.80(2)		
guilleminite			
W(1)–H1A.....O(1)	2.76(6)	O(1)–W(1)–O(4)	83(2)
W(1)–H1B.....O(4)	2.88(6)		
W(2)–H2A.....O(5)	3.00(5)	O(5)–W(2)–O(6)	75(1)
W(2)–H2A.....O(6)	3.15(5)	O(5)–W(2)–O(8)	83(1)
W(2)–H2B.....O(8)	3.03(5)	O(6)–W(2)–O(8)	146(2)

DESCRIPTION OF THE STRUCTURE

Coordination of the cations

There are three unique *U* sites in marthozite (Fig. 1): *U*(1) is surrounded by eight O atoms in a hexagonal bipyramidal arrangement; *U*(2) and *U*(3) are each surrounded by seven O atoms in a pentagonal bipyramidal arrangement. The presence of the uranyl ion, $(UO_2)^{2+}$, with U–O bond lengths of ~1.8 Å (Table 2), indicates that all U in the structure is present as U^{6+}; this result is in accord with the bond-valence sums at the *U* sites (Table 4). There are two unique *Se* sites, each occupied by Se^{4+} and coordinated by three O atoms (*Se*–O ≈ 1.70 Å), with the Se atom displaced above the plane of the O atoms to form a triangular pyramid with Se at the apex; this arrangement is typical for Se^{4+} exhibiting stereoactive lone-pair behavior. The *Cu* site is occupied by Cu, which is bonded to four (H_2O) groups [*Cu*–(H_2O) ≈ 2.0 Å] and two O atoms (*Cu*–O ≈ 2.4 Å) in an octahedral arrangement; the four short bonds are approximately coplanar, a [4 + 2]-coordination that is typical of octahedrally coordinated Cu^{2+} exhibiting Jahn–Teller distortion.

Topology of the structure

The structures of marthozite and guilleminite are based on the topologically identical sheet of ($U\phi_n$) and (SeO_3) polyhedra; their principal structural differences involve the interlayer (interstitial) species. Below, we compare various aspects of the two structures side-by-side in Figures 1 to 4 [(a): marthozite, (b): guilleminite] in order to help understand how distortions in the sheets and the stereochemistry of the two interlayers are related.

The sheet: In both structures, the sheet has the composition [$(UO_2)_3(SeO_3)_2O_2$] and is comprised of chains of edge-sharing ($U\phi_n$) polyhedra extending along [100] that are cross-linked in the [001] direction by (SeO_3) groups (Figs. 1a, b). This sheet is related to the [$(UO_2)_3(PO_4)_2X_2$] sheets in phosphuranylite (*X* = O), upalite and françoisite–(Nd) (*X*$_2$ = O{OH}), dewindtite (*X* = O + additional H), vanmeersscheite (*X* = OH), dumontite (*X* = O), phurcalite and phuralumite (*X* = OH), and althupite (*X*$_2$ = O{OH}) (Burns *et al.* 1996). In guilleminite ($P2_1nm$), there is mirror symmetry at $z = 0$, and the chains of ($U\phi_n$) polyhedra are bilaterally symmetrical (Fig. 1b). In marthozite ($Pbn2_1$), there is no mirror present, and the chains of ($U\phi_n$) polyhedra lack bilateral symmetry; the edge-sharing pentagonal bipyramids are symmetrically distinct, although there is significant pseudosymmetry present (Fig. 1a).

Comparison of the *a* and *c* cell-dimensions of these two minerals shows that marthozite has a shorter repeat along [100] and a longer repeat along [001] than guilleminite. In marthozite, the approximately linear $(UO_2)^{2+}$ groups show a greater departure from alignment along [010] than in guilleminite. These tilts alternate along the chain of ($U\phi_n$) polyhedra in the [100] direction, resulting in a corrugation along [100] in marthozite, consistent with its marginally shorter *a* dimension. Inspection of Figures 1a and 1b indicates that there is no significant contraction within the chain of ($U\phi_n$) polyhedra in the [001] direction; the relative lengthening along [001] in marthozite (relative to guilleminite) must occur by a different mechanism.

Inspection of the *Se* sites relative to the three O atoms of the (SeO_3) groups shows that the Se atom is more centrally positioned relative to the three O atoms in marthozite than in guilleminite. In marthozite, extension of the sheet along [001] is coupled to rotation of the (SeO_3) groups, which in turn is promoted by flexing of the U–O–Se bond angles, resulting in an overall flatten-

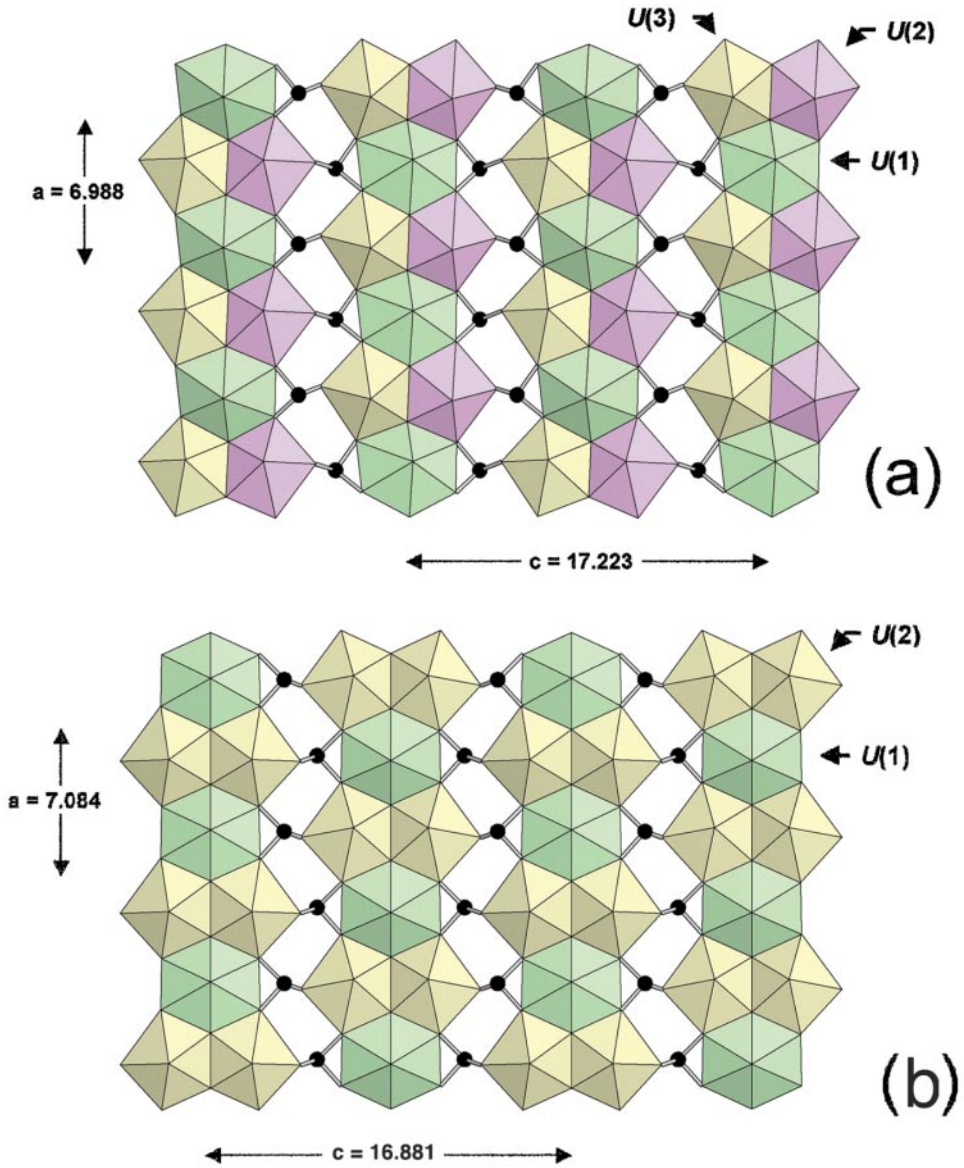

FIG. 1. The structural units of (a) marthozite and (b) guilleminite projected onto (010); Se atoms are shown as small black circles.

ing of the entire sheet in marthozite relative to that in guilleminite (*cf.* Figs. 2a and 2b). In Figure 3, parts of the chain of (UO_n) polyhedra are compared in terms of the bond valences of the U–O(equatorial) bonds. Comparison of all bond valences associated with the pentagonal bipyramids shows that the *U*(2)–*U*(2) dimer in guilleminite has essentially the same bond-valence distribution as the *U*(2)–*U*(3) dimer in marthozite. The key difference between the two structures occurs in the bond valences associated with the hexagonal bipyramid [$U(1)O_8$]. The values of the bond valences are much more evenly distributed around the *U*(1) site in guilleminite [with O(7) and O(9) receiving 0.33 and 0.32 valence units (*vu*), respectively] than around the *U*(1) site in marthozite [with the analogous O(2)–O(5) and O(3)–O(6) pairs of O atoms receiving an average

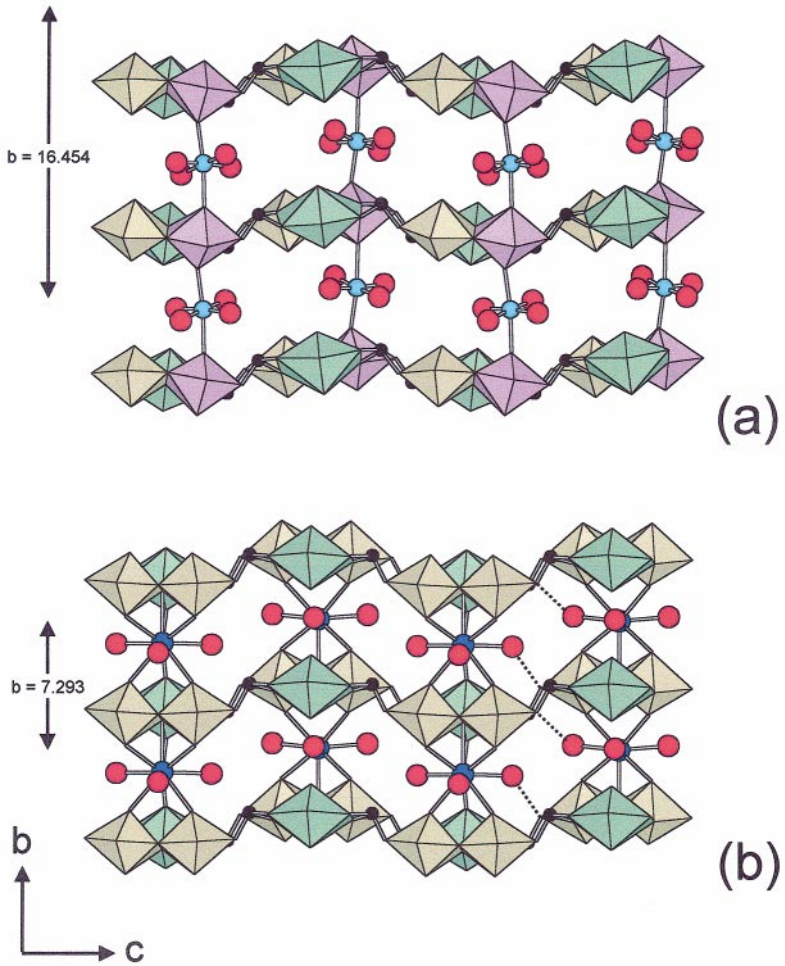

FIG. 2. The crystal structures of (a) marthozite and (b) guilleminite projected down [100] and down an axis 7° from [100], respectively; legend as in Figure 1. Cu^{2+} and Ba are shown as light blue and dark blue circles, respectively, and (H_2O) groups are shown as red circles.

of 0.39 and 0.25 *vu*, respectively]. The two equatorial bonds to *U*(1) oriented along [100] are of nearly equal strength in guilleminite [0.64 and 0.60 *vu*], compared to unequal values [0.61 and 0.76 *vu*, respectively] in marthozite. This asymmetrical distribution of bond valence around the *U*(1) site in marthozite has two consequences: (1) it is responsible for the corrugation along [100] in the (UO_n) polyhedral chain; (2) the O atom at O(14) in marthozite has its bond-valence requirements met solely by contributions from the three neighboring U atoms. In guilleminite, the analogous O atom at O(2) receives only 1.84 *vu* from the neighboring U atoms; however, the interlayer Ba atom contributes an additional 0.17 *vu* to bring the total valence incident at the O(2) site to 2.01 *vu*. Stereochemically, it would be unreasonable for interlayer Cu^{2+} in marthozite to mimic the behavior of the Ba atom in guilleminite, as this would produce an unfavorably close approach of the equatorial (H_2O) groups of the ($Cu\phi_6$) octahedron to the three uranyl O atoms. In this regard, the distinctively different bonding environments of interlayer Cu^{2+} and Ba^{2+} are directly related to the different distortions in the neighboring U–Se sheets in marthozite and guilleminite.

The interlayer: Meshing of the U–Se sheets around the interlayer constituents in marthozite and guilleminite is shown in Figure 2; interlayer (H_2O) groups not bonded to Cu^{2+} in marthozite have been excluded for

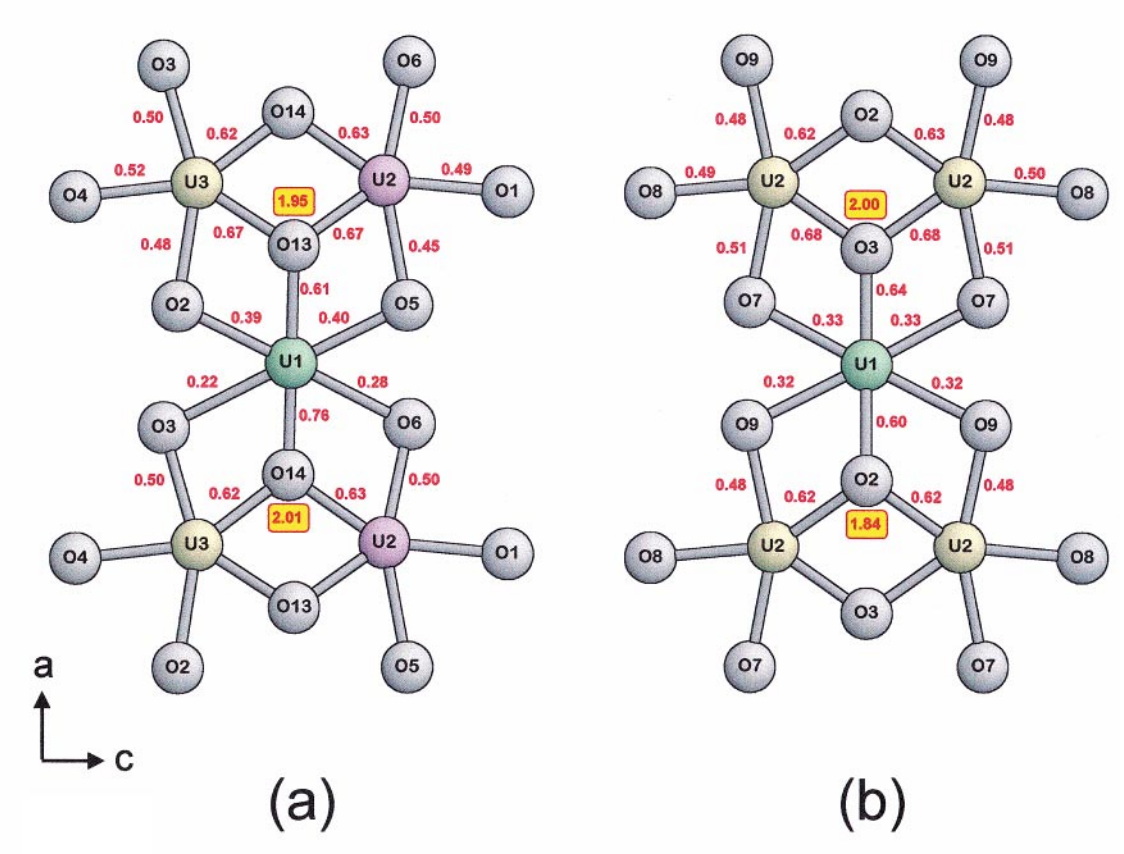

FIG. 3. Linkage of U and O atoms of the structural units of (a) marthozite and (b) guilleminite; bond valences and some bond-valence sums (in yellow boxes) are shown.

simplicity. In marthozite, the repeat distance along [010] is twice that in guilleminite; the ends of the chain of (UO_n) polyhedra have opposing tilts in adjacent sheets, and the marthozite sheet is relatively flattened in the *a*–*c* plane.

In guilleminite, the Ba atom is centrally positioned with respect to the chain of (UO_n) polyhedra (Figs. 2b, 4b), whereas the Cu^{2+} atom in marthozite is located off the pseudo-mirror plane of the chain of (UO_n) polyhedra (Figs. 2a, 4a). Figure 2b shows the guilleminite structure rotated 7° off [100] so that all ligands of the [10]-coordinated Ba site are visible. These ligands involve three interlayer (H_2O) groups, six uranyl O atoms in adjacent sheets, and one O atom at the O(2) site [*cf.* Fig. 3b]. In guilleminite, Ba is nearly equidistant (2.90 – 2.97 Å) from seven O atoms of the structural unit, and closely surrounded by the three interlayer (H_2O) groups in a triangular arrangement (Figs. 2b, 4b). The H_2O groups occur over the topographic lows in the underlying sheet, forming a regular clinomesh of (H_2O) groups along (301) and ($30\bar{1}$). In marthozite, the situation involving Cu^{2+} is very different: there are only two bonds (2.32 and 2.45 Å) between the interlayer Cu^{2+} and uranyl O atoms of the [$U(2)\phi_7$] polyhedra.

The interlayer in marthozite is more expanded than that in guilleminite, and linkage through the long apical bonds to Cu seems to provide only tenuous structural support. Perhaps because of the expanded interlayer, the topography of the sheet in marthozite (Fig. 4a) seems to exert less of a constraint on the positions of the (H_2O) groups than in guilleminite. The separation of adjacent sheets in marthozite is half the repeat distance along [010], 16.454 / 2 = 8.227 Å; the corresponding intersheet separation in guilleminite is equal to the translation along *b* (7.293 Å). Thus although Ba is a much larger cation that Cu^{2+}, the different siting of these two interstitial species in the interlayer results in an intersheet separation in marthozite that is nearly 1 Å greater than that in guilleminite.

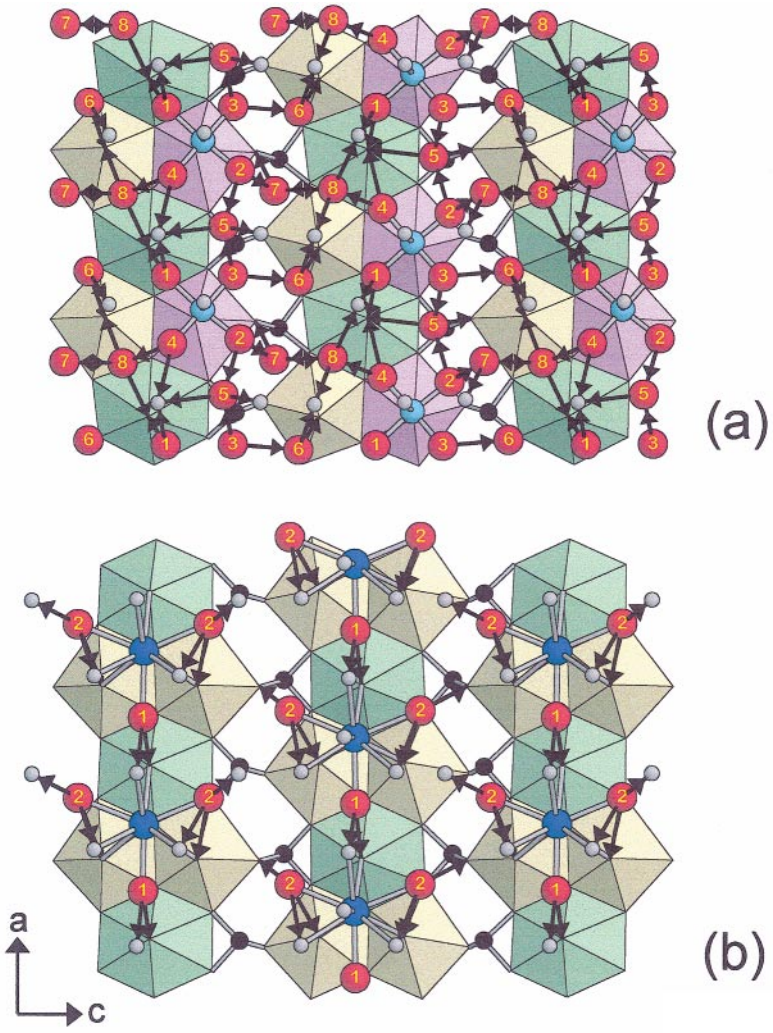

FIG. 4. Hydrogen bonding in (a) marthozite projected onto (010), and (b) guilleminite, projected down an axis 8° from [010]; legend as in Figure 2, H-bond linkages are shown as heavy black lines, the arrows denoting the acceptor anions.

Hydrogen bonding

Several factors commonly combine to make the derivation of H-bonding patterns quite difficult in uranium minerals: (1) The actual H-atoms are not usually observed in final difference-Fourier maps; (2) inadequate correction for absorption, which can result in inaccurately determined positions for the anions in the structure; (3) *apparent* disorder of, or vacancies associated with, interlayer components; (4) calculation of incorrect bond-valences at the uranyl O atoms owing to use of inaccurate bond-valence curves; (5) the occurrence of several possible H-bond acceptor-anions. Although assignment of H bonds can be quite difficult, it is important that this be done, as it is the H bonds that hold adjacent sheets together and control the stability of the mineral. Both guilleminite and marthozite are well-refined structures with fully ordered sheets and fully ordered interstitial constituents. They are suitable candidates for detailed examination of their H bonding, and we present a full description of the proposed H-bonding schemes in each structure.

Inspection of the bond-valence tables for marthozite and guilleminite (Tables 4, 5) shows that the following O atoms have their bond-valence requirements met without any bond-valence contribution from H bond-

ing: (1) those O atoms that bond to three U atoms; (2) those O atoms that bond to two U atoms and one Se atom. The O atoms that bond to one U atom and one Se atom do not receive sufficient bond-valence from these two cations to satisfy their bond-valence requirements, and accordingly, we have designated these O atoms as H-bond acceptors. Inspection of Figure 2 shows that these O atoms, *via* the corrugation of the $[(UO_2)_3(SeO_3)_2O_2]$ sheet along [001], can accept H bonds from the interlayer (H_2O) groups. We have illustrated this relation on the right-hand side of Figure 2b with dashed H-bonds from the W(2) site to the O(8) sites in guilleminite.

In guilleminite, each uranyl O atom receives significantly less than 2 *vu* from its coordinating U atom (1.77–1.87 *vu*), and hence must be a H-bond acceptor; inclusion of the H-bond contribution to the incident bond-valence sums gives a range in values from 1.83 to 2.04 *vu*. In marthozite, only the uranyl O atoms associated with the [U(2)ϕ_7] polyhedron bond to the interstitial Cu^{2+} atom, and incident bond-valence sums at the uranyl O atoms range from 1.58 to 1.74 *vu* from U and interstitial Cu^{2+}; hence all uranyl O atoms not bonded to Cu must be H-bond acceptors, and the resulting bond-valence sums range from 1.73 to 1.91 *vu*.

The strengths of all assigned H-bonds have been partitioned into two groups based on the distances between the donor (O_D) and acceptor O atoms (O_A): O_D–O_A distances of 2.60 to 2.80 Å correspond to a bond valence of 0.2 *vu;* O_D–O_A distances of 2.80 to 3.01 Å correspond to a bond valence of 0.1 *vu*. The H bonds associated with the (H_2O) group at W(2) in guilleminite are more complicated and are discussed in greater detail below. The geometrical indicators of potential H-bonds include a maximum O_D–O_A separation of 3.2 Å and an O_A–O_D–O_A angular range from 70 to 150°. Hydrogen bonding along an edge of the ($Cu^{2+}\phi_6$) octahedron is not considered possible; H bonding along an edge of the ($Ba\phi_{10}$) polyhedron is considered possible (Baur 1972, 1973). In general, the incident bond-valence sums at the uranyl O atoms are somewhat low; this is likely due to slight underestimation in the bond-valence calculation for the short U^{6+}–O_{Ur} bonds using the curves of Burns *et al* (1997). For the structure of rutherfordine (Finch *et al*. 1999), which contains a uranyl O atom that bonds only to U^{6+}, application of this bond-valence curve gives a similar low valence (1.80 *vu* for the uranyl O atom).

Hydrogen bonding in guilleminite

The H-bonding scheme in guilleminite is relatively straightforward. Hydrogen bonds involve the uranyl O atoms above and below the W(1) and W(2) sites at which the interstitial (H_2O) groups occur (Fig. 4b). The H atoms of the (H_2O) group at the W(1) site [H(1A) and H(1B)] link to the acceptor anions O(1) and O(4), with donor–acceptor distances of ~2.8 Å. The W(2) site lies on a special position, and two constituent H atoms occupy only one symmetrically distinct site. This site is ~3.06 Å from three anion sites, O(5), O(6) and O(8), which are feasible H-bond acceptors (Table 6). Bond-valence considerations suggest that all of these anions are probable H-bond acceptors (Table 5), and thus we have represented the H bonding associated with W(2) as a bifurcated bond involving O(5) and O(6), and a single bond involving O(8).

Hydrogen bonding in marthozite

In marthozite, there are eight unique (H_2O) groups occupying the W sites. The (H_2O) groups at the W(1–4) sites are bonded to Cu^{2+}; the O atoms associated with W(5–8) are held in the structure solely by H bonds. It is clear from Table 4 that the four short bonds from Cu^{2+} to W(1–4) provide sufficient bond-valence for the O atoms of the (H_2O) groups, and hence the O atoms of the (H_2O) groups occupying W(1–4) do not function as H-bond acceptors. The H bonds from W(1–4) are directed toward the uranyl O-atoms of *U*(1) and to the O atoms of the (H_2O) groups occupying W(5–8). The H bonds from W(5–8) are directed toward a variety of acceptor anions: (1) uranyl O-atoms of the *U*(1) and *U*(3) polyhedra; (2) other O atoms of (H_2O) groups occupying the W(5–8) sites; (3) sheet O atoms linked to one U atom and one Se atom (Fig. 4a, Tables 4, 6).

The H-bond arrangement in marthozite is very different in character from that in guilleminite. In marthozite, uranyl O-atoms not bonded to Cu^{2+} receive from one to three H-bonds, whereas the uranyl O-atoms of the *U*(2) polyhedron (that bond to Cu^{2+}) receive no H bonds. In guilleminite, each uranyl O-atom receives one bond from Ba and one H bond from an (H_2O) group. In marthozite, if one excludes the possibility of H bonding along the edge of the ($Cu^{2+}\phi_6$) octahedron by one of the (H_2O) groups at W(1 – 4), then the uranyl O-atoms belonging to the {*U*(2)ϕ_7} polyhedron cannot be H-bond acceptors, as the (H_2O) groups at the W(5–8) sites are too distant (≥ 3.47 Å). The low incident bond-valence of 1.73 and 1.74 *vu* at the O(9) and O(10) anions must be a feature of this region of the structure. As indicated in Table 4, the assigned H-bonds result in bond-valence sums from 1.85 to 1.91 *vu* at the uranyl O-atoms of the {*U*(1)ϕ_8} and {*U*(3)ϕ_7} polyhedra.

Each of the four (H_2O) groups at the W(5–8) sites receives two H-bonds, except for W(6), which receives a single H-bond from the (H_2O) group at W(3). However, W(6) is quite far (3.01 and 2.95 Å) from the acceptor anions [O(11) and O(12)], indicating relatively weak (0.1 *vu*) H-bonds and strong (~0.9 *vu*) donor bonds. Reception of a single H-bond from W(3) by W(6) is consistent with the valence-sum rule: 0.9 + 0.9 + 0.2 = 2.0 *vu*; moreover, no other (H_2O) group is sufficiently close to W(6) to act as an additional H-bond donor. For the (H_2O) group at W(8), there are two possible H-bond arrangements; H(8A) could form a H bond either with

the O(7) or O(11) uranyl O-atoms. In the absence of any indication of which arrangement is preferred, we have assigned a disordered configuration (Table 6).

Possible polymorphism in marthozite

In marthozite, the incident bond-valences at all uranyl O-atoms (from the U^{6+} atoms alone) are similarly low. Individual bond-valence contributions on the order of 0.1 to 0.2 *vu* can be provided to these uranyl O-atoms by H bonds or by bonds involving the interstitial Cu^{2+}. From a geometrical perspective, there seems no obvious reason why Cu^{2+} must assume a position between the uranyl O-atoms of the $\{U(2)\phi_7\}$ polyhedra. The separations across the interlayer between opposing uranyl O-atoms of the $\{U(1)\phi_8\}$, $\{U(2)\phi_7\}$ and $\{U(3)\phi_7\}$ polyhedra are 4.75, 4.75 and 4.79 Å , respectively, and there seems no reason why Cu^{2+} could not easily be located between any of the three pairs of opposing uranyl O-atoms. Also, there seems to be little controlling the exact positioning of the four equatorial (H_2O) groups [W(1–4)] bonded to Cu^{2+}, relative to the positions of the uranyl O-atoms.

To test the possibility of Cu^{2+} being located between $\{U(1)\phi_8\}$ or $\{U(3)\phi_7\}$ polyhedra, we collected rapid diffraction-intensity datasets on three other marthozite crystals from the same sample. All three crystals gave the same atomic arrangement as that presented here. Although we were unable to find a different polymorph of marthozite, it is difficult to put a convincing case that the current observed structure is the only possible arrangement in crystal-chemical terms.

"Metamarthozite"

Cesbron *et al.* (1969) reported the occurrence of a phase that forms spontaneously at room temperature by dehydration of marthozite; they named this phase "metamarthozite". This phase is also orthorhombic and has the same translation periods parallel to the $[(UO_2)_3(SeO_3)_2O_2]$ sheet ($a \approx 7.0$, $c \approx 17.2$ Å) as marthozite. The translation perpendicular to the sheet in "metamarthozite" is 15.80 Å, distinctly shorter than the analogous 16.45 Å in marthozite. The separation between adjacent sheets in "metamarthozite" is 15.80 / 2 = 7.90 Å, compared to 8.227 Å in marthozite. The $<Cu–O_{apical}>$ distance in marthozite is 2.385 Å. If *Cu* were similarly positioned between uranyl O-atoms in "metamarthozite", the resulting $<Cu–O_{apical}>$ distance would be ~2.22 Å, and the associated bond-valence would be about 0.23 *vu*, a reasonable contribution to a uranyl O-atom. If this were the case in "metamarthozite", *Cu* would have a different type of coordination than in marthozite, as 2.22 Å is rather short for a typical $<Cu–O_{apical}>$ distance.

Thermogravimetric analysis of marthozite gave an early low-temperature weight loss of 3.05 wt.%, and the X-ray pattern of this partly dehydrated phase is consistent with that of "metamarthozite" (Cesbron *et al*. 1969). The ideal H_2O content for marthozite is 11.06 wt.%. A weight loss of 3.05 wt.% H_2O is consistent with a content of 5.8 H_2O groups in "metamarthozite", suggesting that the correct formula for the latter phase is $Cu^{2+}[(UO_2)_3(SeO_3)_2O_2](H_2O)_6$.

Acknowledgements

We thank Bill Pinch for again providing us with samples of superb quality, Bob Finch, an anonymous referee and Associate Editor Peter C. Burns for their comments on this paper. This work was supported by Natural Sciences and Engineering Research Council of Canada Major Facility Access, Major Equipment and Research grants to FCH.

References

Baur, W.H. (1972): Prediction of hydrogen bonds and hydrogen atom positions in crystalline solids. *Acta Crystallogr.* **B28**, 1456-1465.

_____ (1973): Criteria for hydrogen bonding. II. A hydrogen bond in the edge of a coordination polyhedron around a cation. *Acta Crystallogr.* **B29**, 139-140.

Brown, I.D. & Altermatt, D. (1985): Bond-valence parameters obtained from a systematic analysis of the inorganic crystal structure database. *Acta Crystallogr.* **B41**, 244-247.

Burns, P.C. (1998): CCD area detectors of X-rays applied to the analysis of mineral structures. *Can. Mineral.* **36**, 847-853.

_____, Ewing, R.C. & Hawthorne, F.C. (1997): The crystal chemistry of hexavalent uranium: polyhedron geometries, bond-valence parameters and polymerization of polyhedra. *Can. Mineral.* **35**, 1551-1570.

_____, Miller, M.L. & Ewing, R.C. (1996): U^{6+} minerals and inorganic phases: a comparison and hierarchy of crystal structures. *Can. Mineral.* **34**, 845-880.

Cesbron, F., Oosterbosch, R. & Pierrot, R. (1969): Une nouvelle espèce minérale: la marthozite: uranyl-sélénite de cuivre hydraté. *Bull. Soc. fr. Minéral. Cristallogr.* **92**, 278-283.

Cooper, M.A. & Hawthorne, F.C. (1995): The crystal structure of guilleminite, a hydrated Ba–U–Se sheet structure. *Can. Mineral.* **33**, 1103-1109.

Finch, R.J., Cooper, M.A., Hawthorne, F.C. & Ewing, R.C. (1999): Refinement of the crystal structure of rutherfordine. *Can. Mineral.* **37**, 929-938.

Received October 28, 2000, revised manuscript accepted March 17, 2001.